Electronic Supplementary Material

General Label-Free Mass Spectrometry-Based Assay To Identify Glycosidase Substrate Competence

Gabe Nagy*, Tianyuan Peng*, and Nicola L. B. Pohl**

* Both authors contributed equally

** Corresponding author

Department of Chemistry, Indiana University, Bloomington, IN 47405

Email: npohl@indiana.edu

Phone: 812-855-0298

Fax: 815-855-8300

Table of contents:

Protein purification and expression

SDS-page gel analysis results of purified enzyme; Lane M: Molecular weight marker; Lane 1: purified soluble PF1208 protein monomer (band below), blurry band on top matches the misfolded dimer; Lane 2: purified JL-18 protein (band below), blurry band on top matches misfolded dimer. Over 90% band purity detected for PF1208 (lane 1) & JL-18 (lane 2) using gel imager 3.0 (Bio-Rad, Hercules, CA). JL-18 is the α-galactosidase and PF1208 is the β-mannosidase.
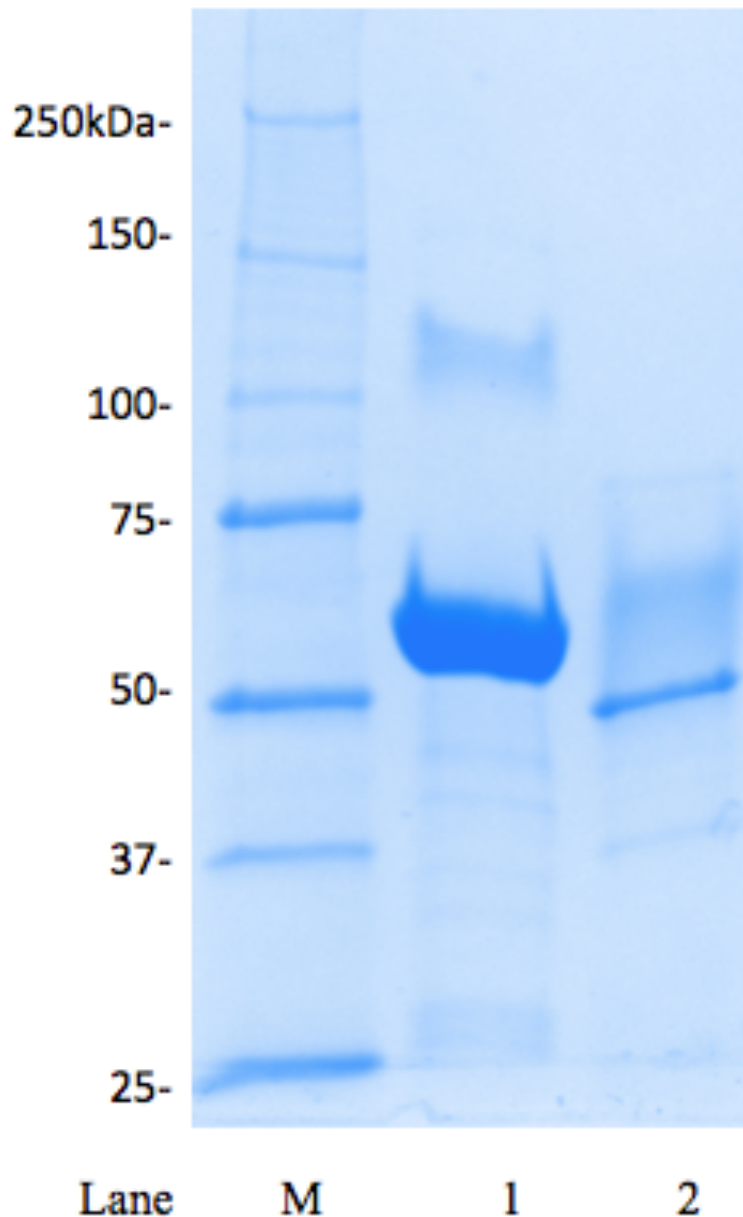

Figure S1. SDS-page gel analysis results of purified enzyme.

Enzymatic activity of JL-18

Commercial 4-nitrophenyl-α-D-galactopyranoside (PNP-galactose) was used for enzyme kinetic measurements to initially test the enzyme. Such nitrophenyl-containing sugars have been often used as part of glycosidase activity assays for kinetic measurements. Amounts of 4-nitrophenol produced were measured with a spectrometer at 405 nm ($\varepsilon=18.1$ mM^{-1} cm^{-1}). Enzyme (2 μl, JL-18, 0.37 mg/ml), 28 μl PNP-mannose substrate (25 mM, 50/50 *v/v* methanol/deionized water) and 20 μl phosphate buffer (pH 7.0) were mixed together in one reaction vial. The reaction mixture was incubated under a range of external temperatures (70-105 °C) for 5 min. After the reaction, the absorbance readings at 405 nm were recorded. Three reactions were conducted in parallel for each temperature. A range of pH conditions (5.0-8.0) were also measured by incubating the reaction mixture at 95 °C for 5 min. Enzyme saturation was measured with a diluted enzyme sample (JL-18, 0.37 mg/ml) reacted at 90 °C, pH 7.0 for 5 min. Aliquots of the reaction mixture were taken out at 30 second time intervals for rate measurements. K_m, k_{cat} and V_{max} values were obtained from the enzyme saturation curve via GraphPad Prism version 6 (La Jolla, CA). K_m and V_{max} values of the enzyme were determined to be 2.55mM and 3.52 mM *para*-nitrophenol released/min/μg enzyme. k_{cat} value is determined to be 1467.4 S^{-1}. The overall catalytic efficiency is 5.75×10^5 M^{-1}S^{-1}. Temperature and pH optimization for JL-18 α-galactosidase test are shown. (A) Average product (nitrophenol) concentration measured at a range of pH (5.0-8.0); (B) Average product (nitrophenol) concentration measured at a range of external temperatures (70-95 °C).
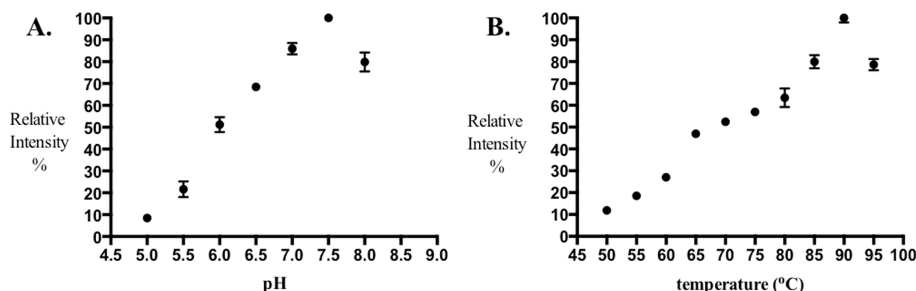

Figure S2: pH and temperature optimization. Relative intensity is based on absorbance at 405 nm.

Recovery ratio test of various monosaccharide-desalting methods

Desalting of all samples before mass spectrometry analysis is necessary because of the presence of large amounts of salts in the enzyme reaction sample. Unlike large hydrophobic samples such as peptides or proteins, monosaccharides are hydrophilic small molecules. Moreover, there presently does not exist any commercially available product that is specifically designed for the desalting of monosaccharides. Several desalting methods (cation/anion exchange resin, boronic acid resin, C18, C4, Carbon graphite, and HILIC-based (hydrophilic interaction liquid chromatography) NuTips) were selected to test their ability to recover the monosaccharides released from the natural products in this study. Briefly, the recovery test is carried out with a 4-nitrophenyl-α-D-mannopyranoside substrate and α-mannosidase (from *Canavalia ensiformis*). A fixed amount of 4-nitrophenyl-α-D-mannopyranoside substrate (10μl, 25 mM) is recovered with each desalting method and reacted with α-mannosidase at 37 °C for 4 hour. While the control samples are the same amount of substrate reacted with α-mannosidase directly at the same condition. Recovery ratio is calculated via comparing the absorbance reading of released nitrophenol at 405 nm. It can be seen that the Carbon NuTip with an eluting buffer of 0.1% formic acid and 90% methanol provided the optimal recovery ratio (bolded row). For these reasons, this was employed for all desalting in this assay. It is important to note that the boronic acid resin was not mass spectrometry compatible because it resulted in numerous salt adducts that leached off the resin seen during analysis. Recovery ratio comparison of different desalting method on nitrophenol substrate. 10 μl of 25 mM 4-nitrophenyl-α-D-mannopyranoside substrate was subject to each desalting method and tested for recovery ratio three times, the average and standard deviation of recovery data is shown in the recovery ratio column. Different eluting buffer systems were used to optimize the recovery ratio of carbon NuTips, where MeOH is methanol, FA is formic acid, ACN is acetonitrile, and Ac is acetate. While this assay is already sensitive in its nanogram quantitation via mass spectrometry, it could be an even more powerful analytical technique if the scientific community were able to improve the lacking recovery/desalting procedures for small hydrophilic molecules like monosaccharides, which would allow for absolute quantitation of any monosaccharide-containing natural product substrate.

Desalting method	Eluting buffer	Recovery ratio
Cation/anion exchange resin	100% MeOH	N/A
Boronic acid resin	0.1 M FA	13.32 % ± 0.35%
C18 ZipTip	0.1% FA, 50% ACN	0.62% ± 0.49%
C4 NuTip	0.1% FA, 50% ACN	0.86% ± 0.26%
Carbon NuTip	0.1% FA, 50% ACN	6.65% ± 1.49%
Carbon NuTip	0.1% FA, 70% MeOH	11.21% ± 1.32%
Carbon NuTip	**0.1% FA, 90% MeOH**	**13.30% ± 0.27%**
HILIC ZipTip	0-10% ACN, 15 mM NH_4Ac (pH 3.5)	N/A

Table S1: Desalting monosaccharide recovery.

Calibration curves, quantitation, and chiral dopant/ligand selection

A calibration curve that plots $ln(R_{relative-fixed})$ versus mole fraction of one analyte versus the other analyte, herein termed as the chiral dopant, can be used to quantitate a binary mixture. Two isomeric analytes can be related to one another through a $R_{iso-fixed}$ term that is the ratio of the respective R_{fixed} values, where a value further from unity signifies a greater degree of chiral discrimination between these two isomers, *M* and *N*, (Eqn. 1).

$$R_{relative-fixed} = \frac{R_{M-fixed}}{R_{N-fixed}} \tag{1}$$

A chiral dopant must be selected that creates the furthest from unity $R_{relative-fixed}$ value. Calibration curves can be created that plot $ln(R_{relative-fixed})$ versus the mole fraction of the analyte of interest versus the chiral dopant, which permits quantitation of the monosaccharide portion of the natural product, similar to other assays but in a label-free manner here with mass spectrometry alone.

A binary mixture of two isomers, *M* and *N*, with a branching ratio referred to as $R_{relative-fixed}$, can be related back to each individual mole fraction Gibbs free energy contribution, where $(\Delta(\Delta G)$ is the change in Gibbs energy, T_{eff} is the average effective temperature of the activated complexes, R is the gas constant, and α_M and α_N are the mole fractions (Eqns. 2–6).

$$ln(R_{relative-fixed}) = \frac{\Delta(\Delta G)}{RT_{eff}} \tag{2}$$

$$\Delta(\Delta G)_{relative} = \alpha_M \cdot \Delta(\Delta G)_M + \alpha_N \cdot \Delta(\Delta G)_N \tag{3}$$

$$ln(R_{relative-fixed}) = \alpha_M \cdot ln(R_M) + \alpha_N \cdot ln(R_N) \tag{4}$$

$$ln(R_{relative-fixed}) = \alpha_M \cdot ln(R_M) + (1 - \alpha_M) \cdot ln(R_N) \tag{5}$$

$$\alpha_{M\ vs\ N} = \frac{\alpha_M}{\alpha_M + \alpha_N} \tag{6}$$

A chiral dopant must be selected that creates the furthest from unity $R_{relative-fixed}$ value. Calibration curves can be created that plot $ln(R_{relative-fixed})$ versus the mole fraction of the analyte of interest versus the chiral dopant, which permits quantitation of the monosaccharide portion of the natural product, similar to other assays but in a label-free manner here with mass spectrometry alone. Once again, the product is considered to be the result of glycosidase hydrolysis plus the chiral dopant, whereas the control is that of no glycosidase hydrolysis plus the chiral dopant. To screen the kinetic competency of the natural product, *R*-group portion, of the substrate, a more qualitative approach is taken. Here, the relative comparison in observed R_{fixed} values between the product and control, for a substrate table, provides insight on which substrates are more or less kinetically competent for the characterized glycosidase. Furthermore, since the monosaccharide unit stays constant for all of these substrates, this assay determines what *R*-groups are most conducive, or kinetically competent, for the binding pocket of a given glycosidase. For this study, a D-aldohexose was selected for the chiral dopant so as to keep the same absolute configuration and aldehyde functional group, as well as ease of use, as the analytes of interest, D-galactose and D-mannose. From our previous work on hexose isomer discrimination with mass spectrometry, it was observed that the D-allose would make the most suitable chiral dopant, since it provided the furthest from unity $R_{relative-fixed}$ value with D-galactose and D-mannose for four fixed ligand combinations (Cu[II]/L-Ser/5'GMP, Mn[II]/L-Asp/L-Phe-Gly, Ni[II]/L-Asp/5'CMP, and Ni[II]/L-Asp/5'GMP). Here, $R_{relative-fixed}$ from Eqn. 2 is defined as (R_{D-gal} / R_{D-all}) and (R_{D-man} / R_{D-all}). With D-allose chosen as a suitable chiral dopant for both D-galactose and D-mannose, the next step was to optimize the fixed ligand combination that would provide the greatest degree of chiral separation. In addition to the above four fixed ligand combinations, a survey of $R_{iso-fixed}$ values was performed for these fixed ligand combinations: Zn[II]/L-Asp/5'GMP, Mn[II]/L-Thr/L-

Phe-Gly, Zn^{II}/L-Thr/5'GMP, and Zn^{II}/L-Trp/5'GMP.From this survey of fixed ligand combinations, it was observed that all the combinations were capable of forming the initial desired trimeric ion complexes and diastereomeric fragment ions, except that the Zn^{II}/L-Thr/5'GMP provided significant secondary fragments and Zn^{II}/L-Trp/5'GMP had one fragment ion in too low of relative abundance for accurate and reproducible measurements, so both of these combinations were not considered for future use. It was seen that the fixed ligand combination of Mn^{II}/L-Thr/L-Phe-Gly (in bold) provided the largest chiral discrimination as represented by $R_{relative-fixed}$ values, so it was selected as the optimal fixed ligand combination to pair with the D-allose chiral dopant. Specifically, the Mn^{II}/L-Thr/L-Phe-Gly fixed ligand combination was chirally doped with 20 nmol ($2x10^{-8}$ moles) of D-allose. Metal, chiral reference, and fixed ligand were kept at the same concentrations as with the standard calibrants. Since Cooks and co-workers have previously determined that branching ratio R_{fixed} values are not concentration dependent, but rather dependent on the mole fraction of one analyte versus the other, this amount of chiral dopant was chosen to maintain a similar signal to noise ratio as with the standards.

Fixed ligand combination	$R_{relative-fixed}$; $\Delta\Delta G$ (kcal/mol) (R_{D-Gal}/R_{D-All})	$R_{relative-fixed}$; $\Delta\Delta G$ (kcal/mol) (R_{D-Man}/R_{D-All})
Cu^{II}/L-Ser/5'GMP	18.72; 4.95	3.51; 2.12
Mn^{II}/L-Asp/L-Phe-Gly	30.60; 5.78	16.90; 4.78
Ni^{II}/L-Asp/5'CMP	6.03; 3.03	14.35; 4.50
Ni^{II}/L-Asp/5'GMP	16.71; 4.76	4.24; 2.44
Mn^{II}/L-Thr/L-Phe-Gly	**33.81; 5.95**	**18.85; 4.96**
Zn^{II}/L-Asp/5'GMP	12.50; 4.27	7.25; 3.35

Table S2: $R_{iso-fixed}$ values for various fixed ligand combinations, with concentrations as follows: 25 μM M^{II}, and 100 μM A, ref, FL.

While it is expected that this curve should be linear, Zhang and co-workers have described that competition effects between two analytes for the formation of the trimeric ion complex will result in non-linear trends. This can only be determined empirically, but can easily be accounted for by fitting a second degree polynomial function to the $ln(R_{binary-fixed})$ versus mole fraction calibration curve. From this "$y = Ax^2 + Bx + C$" curve, "x" can be solved for with the quadratic equation, which calculates the mole fraction of the desired analyte in the presence of the chiral dopant in a binary mixture. Thus, if the moles of the chiral dopant are known, the moles of the desired analyte can be solved. With this information, two five-point calibration curves were constructed that plot $ln(R_{iso-fixed})$ versus mole fraction for D-galactose versus D-allose and D-mannose versus D-allose with the Mn^{II}/L-Thr/L-Phe-Gly fixed ligand combination based on averaged trials. The five mole fraction data points used for each calibration curve are for D-Gal vs. D-All and D-Man vs. D-All are: 0, 0.25, 0.5, 0.75, and 1. Calibration curves were found to be better expressed as a polynomial fit, with "$y = Ax^2 + Bx + C$" equations and R^2 values also presented.
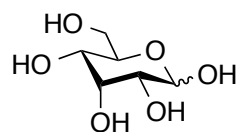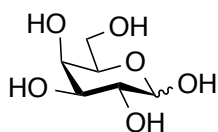
D-allose (D-All)   D-galactose (D-Gal)   D-mannose (D-Man)
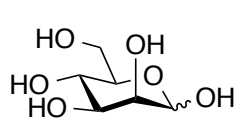
Figure S3: Monosaccharide standards.

Mole fraction D-Gal vs. D-All OR D-Man vs D-All	R_{fixed} value D-Gal vs. D-All	R_{fixed} value D-Man vs. D-All
0.00	0.42 ± 0.00	0.43 ± 0.00
0.25	1.08 ± 0.00	0.84 ± 0.01
0.50	2.13 ± 0.07	1.41 ± 0.04
0.75	4.38 ± 0.02	2.73 ± 0.07
1.00	13.8 ± 0.1	7.9 ± 0.3

Table S3: Mole fraction of D-galactose and D-mannose versus D-allose, respectively.
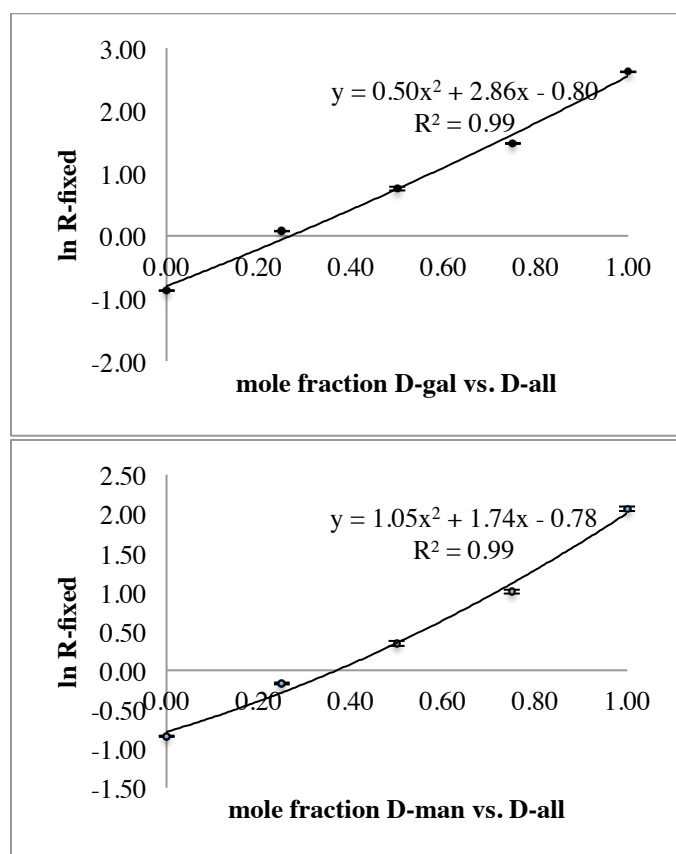
Figure S4: Five point standard calibration curves for the mole fraction of D-galactose versus D-allose (top) and D-mannose versus D-allose (bottom) with the Mn^{II}/L-Thr/L-Phe-Gly fixed ligand combination.

Energetic difference ($\Delta(\Delta G)$) between the D-allose fragment ion versus the D-galactose and D-mannose fragment ions can be graphically determined. This data illustrates that the selection of chiral dopant as well as ligand combination has a tremendous influence on the ability to detect even subtle changes in mole fraction of the analyte of interest, given that the only difference is the axial versus equatorial positioning of a hydroxyl group.

One important note for this assay is that if the initial substrate contains more than one monosaccharide, this technique as described above can be modified. For example, if lactose is the substrate, which is comprised of galactose and glucose in a β-1-4 linkage, both monosaccharides will be released via enzymatic hydrolysis. Thus, when the chiral dopant is added, the observed $ln(R_{fixed})$ is actually composed of three isomers. However, this can easily be accounted for by creating a calibration curve that plots $ln(R_{fixed})$ versus mole fraction of galactose and glucose versus the chiral dopant.

Raw data (R_{fixed}, ΔR_{fixed} (product– control), and amount of monosaccharide cleaved (nanograms)

Note, *n/a* denotes that the product and control were too similar (or standard deviations too great in magnitude) to permit calculations.
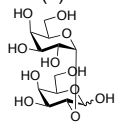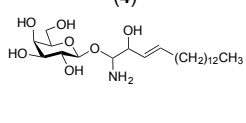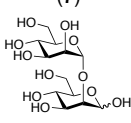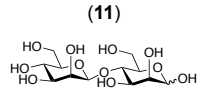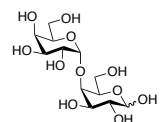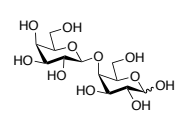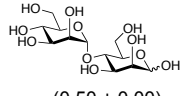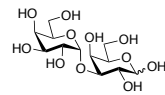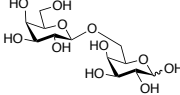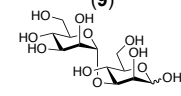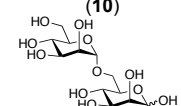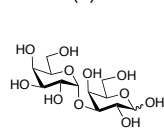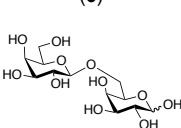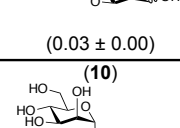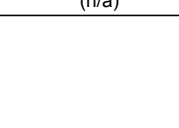
Enzyme	α-galactosidase (JL-18 from *Thermus thermophilus*)	β-galactosidase (*Escherichia coli*)	α-mannosidase (*Canavalia ensiformis*)	β-mannosidase (PF1208 from *Pyrococcus furiosus*)
Substrate and raw R_{fixed} values	**(1)** (0.47 ± 0.01)	**(4)** (0.48 ± 0.00)	**(7)** (0.67 ± 0.01)	
	(2) (0.47 ± 0.01)	**(5)** (0.50 ± 0.00)	**(8)** (0.50 ± 0.00)	**(11)** (0.49 ± 0.01)
			(9) (0.46 ± 0.00)	
	(3) (0.49 ± 0.01)	**(6)** (0.45 ± 0.01)	**(10)** (0.46 ± 0.00)	

Figure S5: Raw R_{fixed} values for each substrate for their respective glycosidases.
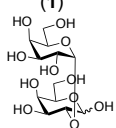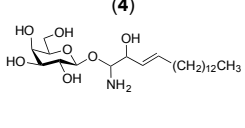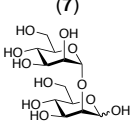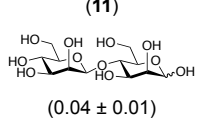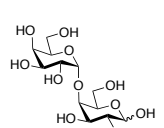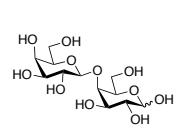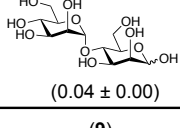
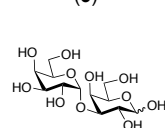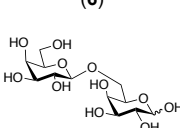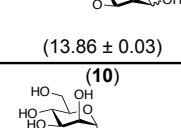| Enzyme	α-galactosidase (JL-18 from *Thermus thermophilus*)	β-galactosidase (*Escherichia coli*)	α-mannosidase (*Canavalia ensiformis*)	β-mannosidase (PF1208 from *Pyrococcus furiosus*)
Substrate and ΔR_{fixed} (product – control)	(**1**) (0.06 ± 0.01)	(**4**) (0.05 ± 0.01)	(**7**) (0.24 ± 0.02)	(**11**) (0.04 ± 0.01)
	(**2**) (0.03 ± 0.01)	(**5**) (0.03 ± 0.01)	(**8**) (0.04 ± 0.00)	
			(**9**) (0.03 ± 0.00)	
	(**3**) (n/a)	(**6**) (n/a)	(**10**) (n/a)	

Figure S6: Raw ΔR_{fixed} values.
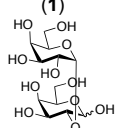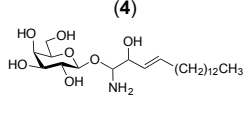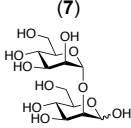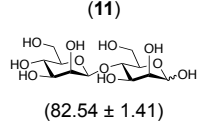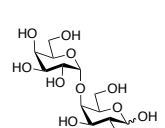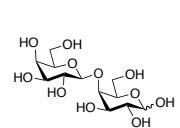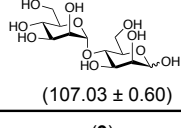
Enzyme	α-galactosidase (JL-18 from *Thermus thermophilus*)	β-galactosidase (*Escherichia coli*)	α-mannosidase (*Canavalia ensiformis*)	β-mannosidase (PF1208 from *Pyrococcus furiosus*)
Substrate and monosaccharide cleaved (nanograms)	**(1)** (65.51 ± 0.89)	**(4)** (99.97 ± 0.56)	**(7)** (550.35 ± 5.14)	**(11)** (82.54 ± 1.41)
	(2) (75.33 ± 1.44)	**(5)** (74.32 ± 0.66)	**(8)** (107.03 ± 0.60) **(9)** (13.86 ± 0.03)	
	(3) (n/a)	**(6)** (n/a)	**(10)** (n/a)	

Figure S7: Nanograms recovered of monosaccharides.

MS^1 spectrum for α-1-2 mannobiose substrate product

Desired trimeric ion complex formation at 575 m/z. Common ions seen are 403 m/z [A+L-Phe-Gly+H]$^+$, 445 m/z [(L-Phe-Gly)$_2$+H]$^+$, and others which are discussed earlier, where A is the monosaccharide analyte (D-man plus the chiral dopant D-all).
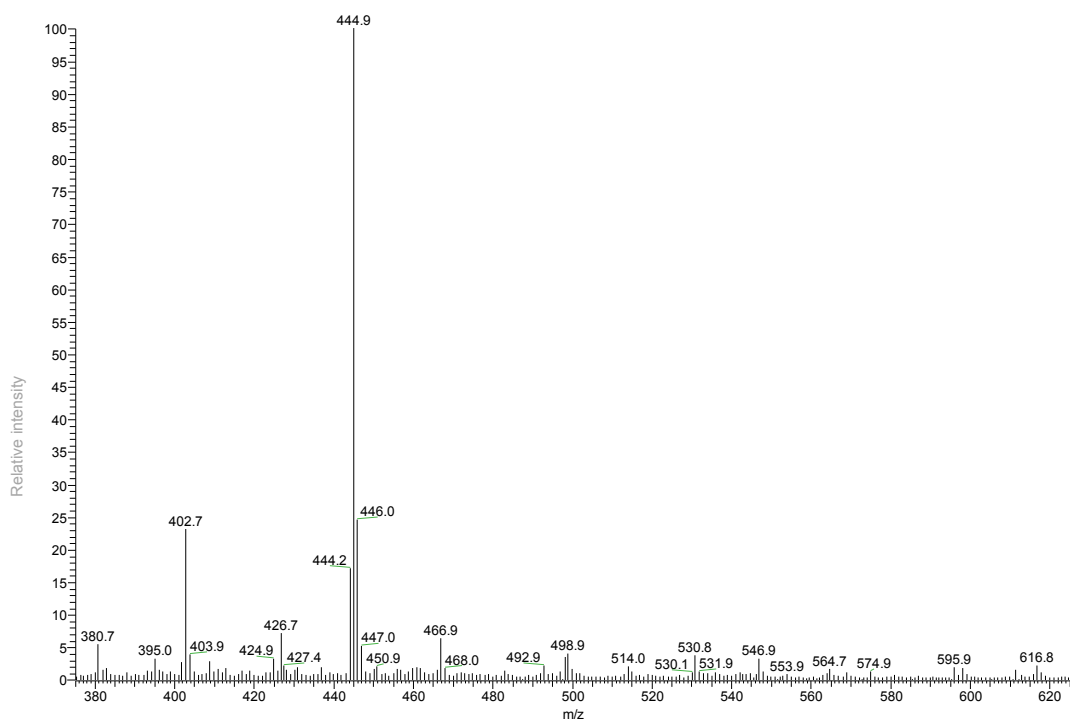

Figure S8: MS^1 spectrum for α-1-2 mannobiose substrate cleaved with α-mannosidase.

Evidence of disaccharide substrate still present post desalting

While it is expected that the enzyme efficiency will never be 100%, the presence of remaining disaccharide would rule out the possibility that recovery issues during desalting are the cause of no recovered monosaccharide being observed. In the negative mode precursor scan of one of the substrate products, the 341 *m/z* ion was observed that corresponds to the deprotonated disaccharide. Upon fragmentation in the negative mode of this deprotonated disaccharide, the common fragment ions were seen at 161, 179, and 221 *m/z*.
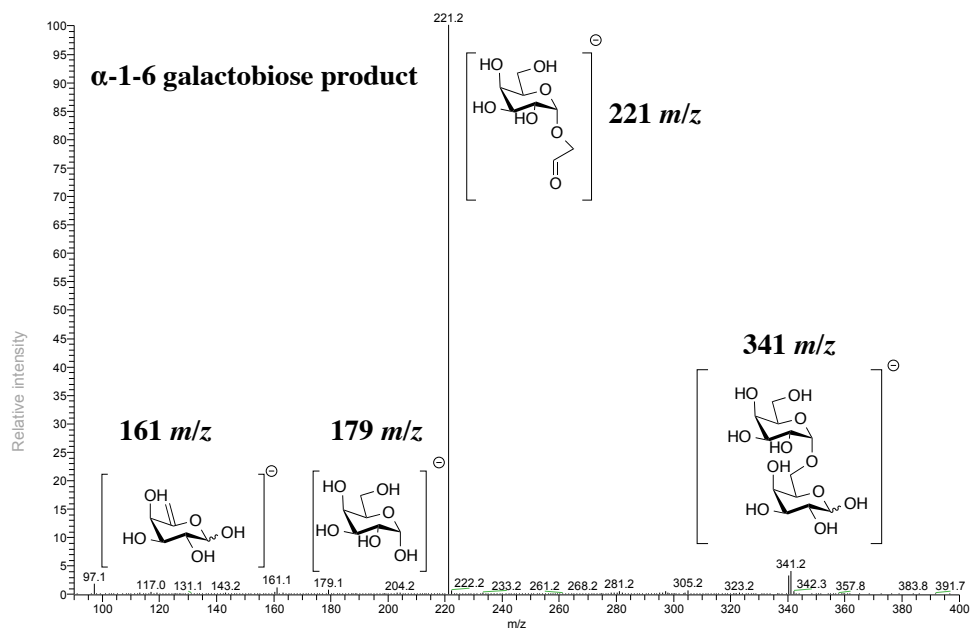

Figure S9: Negative ion mode of α-1-6 galactobiose cleaved with α-galactobiose.
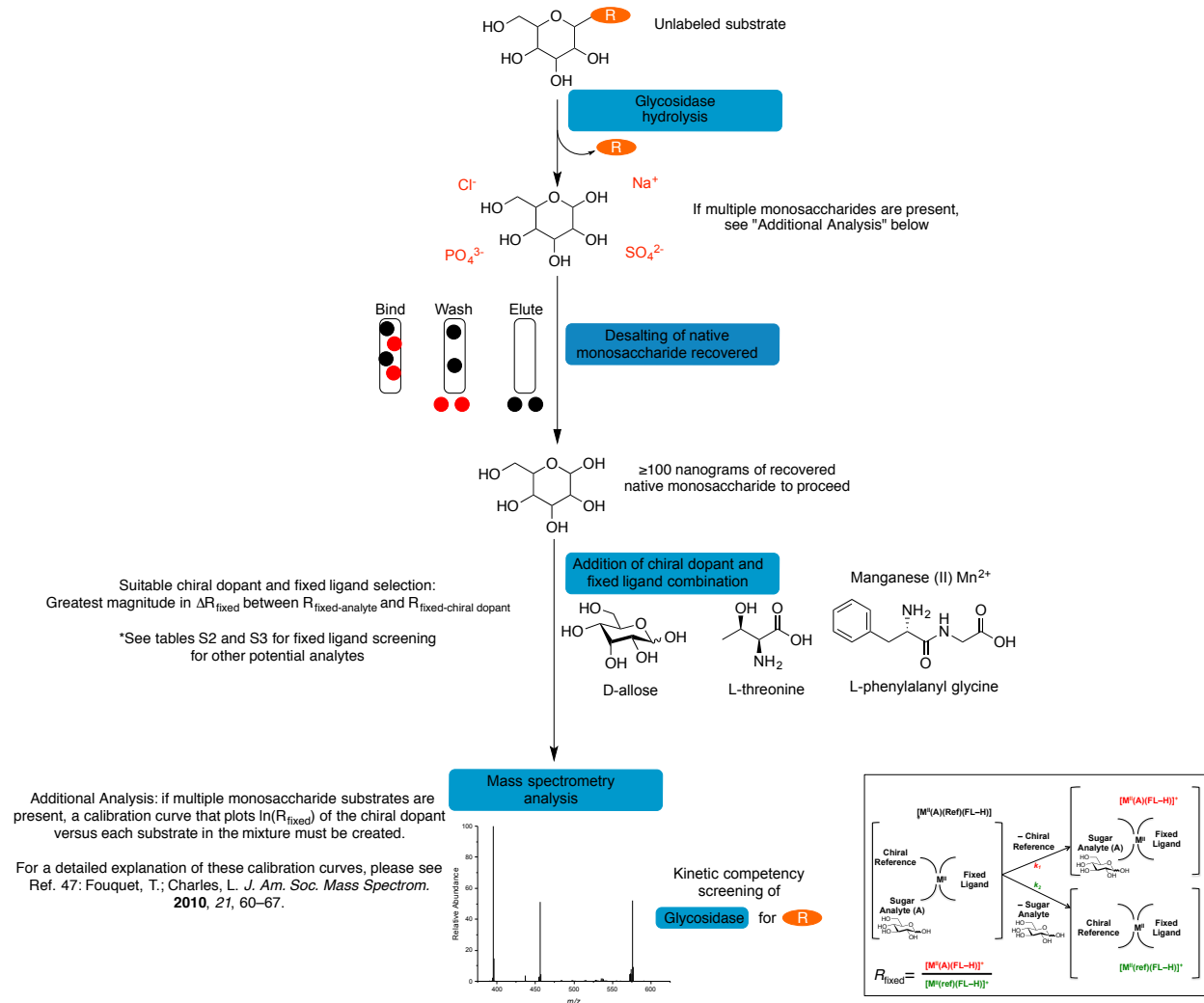
Assay implementation workflow diagram

Figure S10. Workflow diagram of the present glycosidase assay. All conditions cited are presented in either the experimental section of the manuscript or this Supporting Information.